Arabian Journal of Chemistry (2019) 12, 1260–1267

King Saud University

Arabian Journal of Chemistry

www.ksu.edu.sa
www.sciencedirect.com

ORIGINAL ARTICLE

New flavone and phenolic esters from *Callistemon lanceolatus* DC: Their molecular docking and antidiabetic activities

Syed Nazreen [a], Mohammad Sarwar Alam [a,*], Hinna Hamid [a], Abhijeet Dhulap [b], Mohammad Mahboob Alam [a], Sameena Bano [a], Saqlain Haider [a], Mohammad Ali [c], K.K. Pillai [d]

[a] *Department of Chemistry, Faculty of Science, Jamia Hamdard (Hamdard University), New Delhi 110 062, India*
[b] *CSIR Unit for Research and Development of Information Products, Pune 411038, India*
[c] *Department of Phytochemistry and Pharmacognosy, Faculty of Pharmacy, Jamia Hamdard (Hamdard University), New Delhi 110 062, India*
[d] *Department of Pharmacology, Faculty of Pharmacy, Jamia Hamdard (Hamdard University), New Delhi 110 062, India*

Received 30 August 2013; accepted 6 November 2014
Available online 18 November 2014

KEYWORDS

Callistemon lanceolatus;
Flavone;
Phenolic esters;
PPAR-γ;
Antidiabetic

Abstract Phytochemical investigation of the antidiabetic chloroform fraction of the ethanolic extract obtained from the aerial parts of *Callistemon lanceolatus* DC led to the isolation of three new phytoconstituents, one flavone, 8-(1″-hydroxyisopranyl)-5,6-dihydroxy-7,4′-dimethoxy flavone (**1**) and two phenolic esters, 2,3,4-trihydroxyphenethyl tetracontanoate (**2**) and 2,3,4-trihydroxyphenethyl tetracontanoate-4-β-xylopyranoside (**3**). The isolated compound **1** exhibited significant *in vivo* blood glucose lowering effect comparable to the standard drugs Pioglitazone and Rosiglitazone in streptozotocin induced diabetic rats without causing any toxic effect on the pancreas and liver. Compound **1** showed a glide score of −7.89 against PPAR-γ target in molecular docking studies which is significantly higher than the glide score of reference molecule Rosiglitazone (glide score of −5.77). Compound **1** also exhibited moderate *in vitro* PPAR-γ transactivation activity of 48.52% in comparison with standard drugs rosiglitazone and pioglitazone, which showed a transactivation activity of 80.47% and 65.27%, respectively.

* Corresponding author. Tel.: +91 9717927759; fax: +91 11 26059663.
E-mail address: msalam@jamiahamdard.ac.in (M.S. Alam).
Peer review under responsibility of King Saud University.

Production and hosting by Elsevier

1. Introduction

The genus *Callistemon* belongs to family Myrtaceae and comprises over 30 species. These are woody aromatic trees or shrubs and widely distributed all over the world (Anonymous, 1992). The plant is used for ornamental purposes, and has applications in folk medicine as antidiabetic

http://dx.doi.org/10.1016/j.arabjc.2014.11.029
1878-5352

(Nazreen et al., 2011), antimicrobial, antiinflammatory, antistaphylococcal, and antithrombin (Kobayashi et al., 2006; Gomber and Saxena, 2007; Saxena and Gomber, 2006; Chistokhodova et al., 2002). It is also used for nematicidal, larvicidal and pupicidal effects (Sangwan et al., 1990). Previous phytochemical studies on different parts of *Callistemon lanceolatus* (commonly known as Red bottlebrush) have led to the isolation of *C*-methyl flavonoids, triterpenoids, tannins and phloroglucinol derivatives (Wrigley and Fagg, 1993; Huq and Misra, 1997; Wollenweber et al., 2000; Younes, 1975). In our earlier studies we have reported the isolation of two new antidiabetic flavones from the chloroform fraction of the ethanolic extract of this plant (Nazreen et al., 2012). In continuation to our earlier studies, we report herein the presence of a new flavone and two new phenolic esters from the chloroform fraction of the ethanolic extract of this plant. These isolated compounds have been evaluated for *in vivo* antidiabetic potential, molecular docking study and *in vitro* Peroxisome Proliferator Activated Receptor (PPAR-γ) transactivation activity.

2. Experimental

2.1. General

Melting points were determined on Veego VMP-III and were uncorrected. UV spectra were measured on DV 20 Spectroscan spectrophotometer. IR spectra were recorded on Bruker spectrometer using KBr disc. ^{1}H NMR, ^{13}C NMR and 2D NMR were recorded on a Bruker AM-400 (400 MHz) spectrometer with TMS as the internal standard and chemical shifts are reported in parts per million relative to $CDCl_3$ (7.27 ppm for ^{1}H and 77.23 for ^{13}C). Mass spectra were recorded on a Jeol JMS-D 300 instrument fitted with a JMS 2000 data system at 70 eV using Argon/Xenon as the FAB gas. All solvents were of analytical grade (Merck). Thin Layer Chromatography (TLC) was performed on precoated plates (Silica gel 60 F_{254}, Merck) and Silica gel (60–120 mesh, Merck) was used for column chromatography. Pioglitazone and Rosiglitazone were procured from Ranbaxy Laboratories, Gurgaon with purity 97.4%.

2.2. Plant material

The aerial parts of *C. lanceolatus* DC were collected from Saket Nursery, New Delhi in March 2010 and authenticated by Dr. H. B. Singh, Taxonomist, National Institute of Science Communication and Information resources, New Delhi. A voucher specimen (No. 1386/188) has been deposited in the author's laboratory.

2.3. Extraction and Isolation

The air dried and powdered aerial parts of *C. lanceolatus* DC (5 kg) were extracted with 95% ethanol in a Soxhlet apparatus. The ethanolic extract was concentrated under reduced pressure to yield a brown viscous mass (550 g). The ethanolic extract was fractionated with petroleum ether (3×1.0 L), $CHCl_3$ (3×1.0 L), and MeOH (3×1.0 L) to furnish petroleum ether fraction (200 g), $CHCl_3$ fraction (150 g) and MeOH fraction (200 g). The isolation of the compounds has been performed at room temperature (25–30 °C). The chloroform fraction was column chromatographed (CC) over silica gel (60–120 mesh, 1000 g) and eluted with petroleum ether–$CHCl_3$ gradient system from 100:0 to 0:100 to give two crude fractions (1–2). Fraction 1 (50 g) obtained from petroleum ether–$CHCl_3$ (4:6) was further CC over silica gel (60–120 mesh) eluting with same solvent to afford compound **1** which was purified by crystallization with $CHCl_3$–MeOH (80 mg; R_f: 0.34; petroleum ether–$CHCl_3$, 9.5:0.5). Fraction 2 (65 g) obtained from petroleum ether–$CHCl_3$ (3:7) was subjected to CC over silica gel (60–120 mesh) to yield two sub fractions (2a–2b). Fraction 2a when recolumned over silica gel (60–120 mesh) and eluted with same solvent, followed by crystallization in $CHCl_3$–MeOH yielded compound **2** (102 mg; R_f: 0.83; *n*-hexane–EtOAc, 3.5:1.5). Fraction 2b was further CC and recrystallized to yield **3** (90 mg; R_f: 0.42; *n*-hexane–EtOAc, 3.5:1.5).

2.3.1. Compound *1*

Yellow crystals; m.p. 135–136 °C; UV (MeOH) λ_{max}: 286, 323 nm; IR (KBr) υ_{max} (cm^{-1}): 3432 (OH), 1670 (C═O), 1075 (C—O); ^{1}H and ^{13}C NMR ($CDCl_3$): see Table 1; FAB MS (positive): *m/z* 400 $[M]^+$ (calcd 400.42 for $C_{22}H_{24}O_7$), 313 $[M\text{-}C_5H_{11}O]^+$, 166 $[181\text{-}Me]^+$, 117 $[132\text{-}Me]^+$.

2.3.2. Compound *2*

Silver colored crystals; m.p. 79–80 °C; UV (MeOH) λ_{max}: 278 nm; IR (KBr) υ_{max} (cm^{-1}): 3460 (OH), 1729 (C═O), 1178 (C—O); ^{1}H and ^{13}C NMR ($CDCl_3$): see Table 2; FAB MS (positive): *m/z* 744 $[M]^+$ (calcd 744.66 for $C_{48}H_{88}O_5$).

2.3.3. Compound *3*

Orange flakes; m.p. 88–89 °C; UV (MeOH) λ_{max}: 264 nm; IR (KBr) υ_{max} (cm^{-1}): 3437 (OH), 1722 (C═O), 1015 (C—O); ^{1}H and ^{13}C NMR ($CDCl_3$): see Table 2; FAB MS (positive): *m/z* 876 $[M]^+$ (calcd 876.66 for $C_{53}H_{96}O_9$).

2.3.3.1. Acid hydrolysis of 3. Compound **3** was refluxed with 2 N HCl in 80% MeOH for one hour. After cooling, the reaction mixture was poured into crushed ice, and the hydrolysate was then extracted with EtOAc to give the aglycone, compound **2**. The sugar in the concentrated water-soluble portion was compared with standard sugars on a TLC plate with *n*-BuOH–EtOAc–iso-PrOH–AcOH–H_2O (7:20:12:7:6). The sugar was identified as xylose, $R_f = 0.47$.

2.4. Antidiabetic activity

The antidiabetic activity was performed in streptozotocin (STZ) induced diabetic rats as per the previously reported method (Nazreen et al., 2011).

2.4.1. Experimental protocol

The rats were divided into seven groups comprising of five animals each.

Group I: Control rats receiving 0.1 M citrate buffer (pH 4.5).
Group II: Diabetic controls receiving STZ (60 mg/kg b.w.) intraperitoneally.

Group III: Diabetic rats given compound **1** (40 mg, equimolar to standard drug Pioglitazone) in aqueous solution orally.
Group IV: Diabetic rats given compound **2** (75.23 mg, equimolar to standard drug Pioglitazone) in aqueous solution orally.
Group V: Diabetic rats given compound **3** (88.58 mg, equimolar to standard drug Pioglitazone) in aqueous solution orally.
Group VI: Diabetic rats given standard drug pioglitazone (36 mg/kg b.w.) in aqueous solution orally.
Group VII: Diabetic rats given standard drug rosiglitazone (36 mg/kg b.w.) in aqueous solution orally.

The compounds (**1**–**3**) were administered a single dose on the 1st day and the blood glucose level was measured on the 1st, 7th and 15th day of the experiment as per standard protocols by glucose oxidase method (Dahlqvist, 1961).

At the end of the experimental period, the rats were anaesthetized and sacrificed by cervical dislocation. Organs (pancreas and liver) were removed for histopathological evaluation.

2.5. Molecular docking study

Molecular docking studies involve mainly protein selection & preparation, grid generation, ligand preparation, docking & further analysis of docking studies. Schrodinger Software was mainly used for all the above steps. Protein with Accession number 3CS8 was selected and downloaded from Protein Data Bank, and is reported to bind with the drug Rosiglitazone. The protein was imported, optimized, minimized while removing unwanted molecules and other defects reported by the software. Molecules drawn in 3D form were refined by LigPrep module. The molecules were subjected to OPLS-2005 force field to generate single low energy 3-D structure. Docking study was done using Extra precision and Write XP descriptor information. This generates favourable ligand poses which are further screened through filters to examine spatial fit of the ligand in the active site. Ligand poses which pass through initial screening are subjected to evaluation and minimization of grid approximation. Scoring is then done on energy minimized poses to generate glide score.

2.6. PPAR-γ transactivation assay

Human embryonic kidney (HEK) 293 cells were cultured in DMEM with 10% heat inactivated foetal bovine serum in a humidified 5% CO_2 atmosphere at 37 °C. Cells were seeded in 6-well plates the day before transfection to give a confluence of 70–80% at transfection. Cells grown in Dulbecco's Modified Eagle's Medium (DMEM) were inoculated in 96-well plate containing 60,000 cells/well. Cells were transfected with 2.5 μL of Peroxisome Proliferator Response Element-Luciferase (PPRE-Luc), 6.67 μL of PPAR-γ, 1.0 μL of Renilla and 20 μL of Lipofectamine. Following 5 h after transfection, cells were treated with compound (10 μM) for 24 h and then collected with Cell Culture Lysis buffer. Luciferase activity was monitored on luminometer (Perkinelmer, USA) using the luciferase kit (Promega) according to the manufacturer's instructions. Rosiglitazone and Pioglitazone were used as standards.

2.7. Statistical analysis

Data was analysed by GraphPad Instat 3.1 software by one way ANOVA followed by Dunnett's 't' test ($n = 5$), $^{*}p < 0.05$, $^{**}p < 0.01$ significant from diabetic control.

3. Results and discussion

3.1. Structure elucidation

Compound **1** was isolated as yellow crystals and gave positive Shinoda test for flavonoids. Its UV absorption maxima at 286 and 323 nm were typical of substituted flavones (Boue et al., 2003). The +ve FAB mass spectrum exhibited a molecular ion peak at m/z 400 consistent with the molecular formula of a flavone, $C_{22}H_{24}O_7$. The other prominent ion peaks appeared at m/z 313 $[M\text{-}C_5H_{11}O]^+$, 181 $[C_8H_5O_5]^+$, 166 $[C_8H_5O_5\text{-}Me]^+$, 132 $[C_9H_8O]^+$, 117 $[C_9H_8O\text{-}Me]^+$ supporting the existence of two methoxy moiety in the molecule. The IR spectrum revealed absorption bands at 3432 cm^{-1} (OH), 1670 cm^{-1} (C═O) and 1075 cm^{-1} (C─O) functionalities. The ^1H NMR spectrum showed the presence of four aromatic protons (ring B) at δ_H 7.83 (d, $J = 8.2$ Hz, H-2′, H-6′) and δ_H 7.02 (d, $J = 8.8$ Hz, H-3′, H-5′) and two methoxy groups at δ_H 3.92 (6H, s) forming an AA′XX′ system. The presence of two aromatic OH groups at δ_H 12.91 (s, 5-OH) and δ_H 9.92 (s, 6-OH) and a olefinic proton at δ_H 6.57 (s, H-3) indicated 5,6-dihydroxylated pattern for ring A of flavone skeleton. The presence of α-hydroxy-γ,γ-dimethylpropyl group was supported by proton signals at δ_H 3.85 (1H, t, $J = 7.2$ Hz, H-1″), δ_H 2.21 (1H, m, H-3″), δ_H 1.25 (2H, brs, H-2″), δ_H 6.48 (1H, s, 1″-OH), δ_H 0.88 (3H, d, $J = 8.8$ Hz, H-4″) and δ_H 0.81 (3H, d, $J = 8.4$ Hz, H-5″) and carbon signals at δ_C 89.33, 31.94, 29.71, 8.57, 7.29 respectively in the ^{13}C NMR spectrum. The ^1H-^1H COSY spectrum of **1** showed correlations of H-1″ (δ_H 3.85) with H_2-2″ (δ_H 1.25) and H-3″(δ_H 2.21); H-4″ (δ_H 0.88) with H-3″(δ_H 2.21), H_3-5″(δ_H 0.81) and H_2-2″ (δ_H 1.25) and H-2' (δ_H 7.83) with H-3' (δ_H 7.02) and H-6' (δ_H 7.83); H-3' (δ_H 7.02) with H-2' (δ_H 7.83) and H-5' (δ_H 7.02). The long-range ^1H–^{13}C correlations (HMBC) of H-3 (δ 6.57) with C-2 (δ 163.60), C-1′ (δ 123.75), C-4 (δ 182.40), C-10 (δ 105.32) indicated that there is a proton at C-3. The presence of two hydroxyl groups at C-5 and C-6 is based on the long range ^1H–^{13}C correlations which showed correlations of 5-OH (δ 12.91) with C-5 (δ 162.38), C-6 (δ 155.93), C-10 (δ 105.32) while 6-OH (δ 9.92) revealed correlations with C-6 (δ 155.93), C-5 (δ 162.38), C-7 (δ 163.86). The attachment of two methoxy groups at C-7 and C-4′ is evident from the long range correlations observed between δ 3.92 (7-OMe) with C-7 (δ 163.86), C-6 (δ 155.93), C-8 (δ 123.87) and δ 3.92 (4′-OMe) with C-4′ (δ 162.60). By analogy, the side chain at C-8 could be deduced from the long-range ^1H–^{13}C correlations between H-1″ (δ 3.85) with C-8 (δ 123.87), C-9 (δ 158.76), C-7 (163.86); H-2″ (δ 1.25) with C-8 (δ 123.87), C-4″ (δ 8.57), C-5″ (δ 7.29) (Fig. 1). Thus, the compound **1** was identified as *8-(1″-hydroxyisopranyl)-5,6-dihydroxy-7,4'-dimethoxy flavone*.

Compound **2** isolated as white shiny crystals exhibited a molecular ion peak at m/z 744 (calcd 744.66) in its +ve FAB MS, calculated for the molecular formula $C_{48}H_{88}O_5$. It showed UV absorption maxima (MeOH) at 278 nm, and characteristic IR absorption bands at 3460, 1729 and 1178 cm^{-1} for

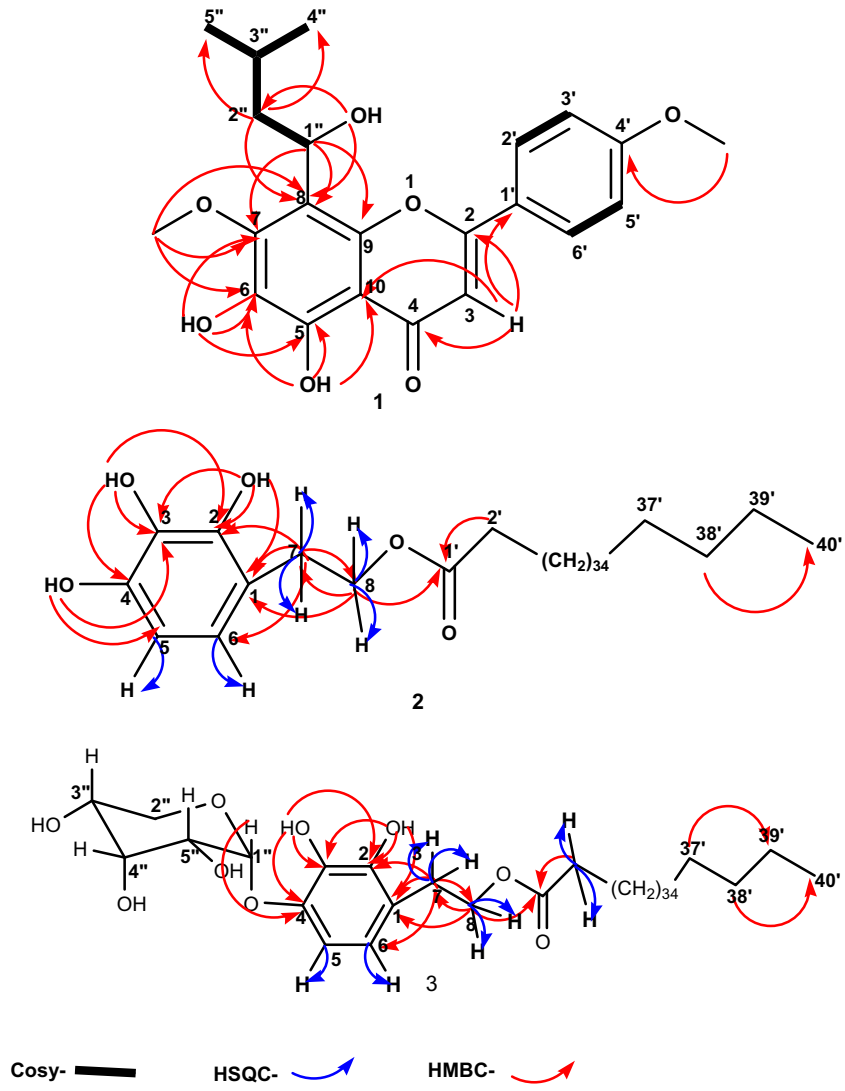

Figure 1 COSY, HSQC and HMBC correlations of compounds **1**–**3**.

hydroxy, carbonyl and ether functionalities, respectively. The ^{1}H NMR spectrum of **2** showed the presence of only two aromatic protons at δ 7.07 (1H, d, J = 8.4 Hz, H-6) and δ 6.76 (1H, d, J = 8.4 Hz, H-5) indicating the aromatic ring is tetra-substituted. The signals of a long alkyl side chain appeared at δ 2.85 (2H, t, J = 7.2 Hz, H_2-7), 4.23 (2H, t, J = 7.2 Hz, H_2-8), 2.27 (2H, t, J = 7.6 Hz, H_2-2′), 1.60 (74 H, brs, $37 \times CH_2$) for methylene protons. A three proton signal appeared at δ 0.88 (3H, t, J = 6.3 Hz, Me-40′) for terminal methyl protons. This data was supported by ^{13}C NMR spectrum which exhibited signals at δ 34.38 (C-7), δ 64.97 (C-8), 34.29 (C-2′), δ 31.94–22.71 ($37 \times CH_2$) and δ 14.41 (Me-40′). The ^{13}C NMR spectrum also revealed downfield signals at δ 173.97 for carbonyl carbon (C-1′), δ 156.21, 156.05 & 154.26 for three oxygenated aromatic carbons (C-4, C-3, C-2) and δ 129.99 (C-6) & 115.33 (C-5) for unsubstituted aromatic carbons. Assignment of each substituent in the aromatic ring was determined by HSQC and HMBC correlations (Fig. 1). From the HSQC spectrum, the aromatic protons H-6 (δ 7.07) showed correlation with C-6 (δ 129.99), H-5 (δ 6.76) with C-5 (115.33), benzylic protons H_2-7 (δ 2.85) with C-7 (δ 34.38), oxygenated methylene protons H_2-8 (δ 4.23) with C-8 (δ 64.97), methylene protons H_2-2′ (δ 2.27) with C-2′ (δ 34.29), remaining seventy four methylene protons (δ 1.60) with C-3′ to C-37′ (δ 31.94–22.71) and terminal methyl protons H_3-40′ (δ 0.88) with C-40′ (δ 14.41). The presence of three hydroxyl groups at C-2, C-3 and C-4 was determined from the long-range ^{1}H–^{13}C correlations (HMBC) which showed interactions of 2-OH (δ 9.42) with C-2 (δ 154.26), C-3 (δ 156.05), C-1 (δ 130.05); 3-OH (δ 10.82) with C-3 (δ 156.05), C-2 (δ 154.26), C-4 (δ 156.21); 4-OH (δ 11.58) with C-4 (δ 156.21), C-3 (δ 156.05), C-5 (δ 115.33). The protons H_2-7 (δ 2.85) exhibited HMBC correlations with C-1 (δ 130.05), C-2 (δ 154.26), C-6 (δ 129.99), C-8 (δ 64.97); H_2-8 (δ 4.23) with C-7 (δ 34.38), C-1 (δ 130.05), C-1′ (δ 173.97); H_2-2′ (δ 2.27) with C-1′ (δ 173.97), C-3′ to C-37′ (δ 31.94–22.71). Thus, the compound was characterized as *2,3,4-trihydroxyphenethyl tetracontanoate*.

Compound **3** was isolated as orange flakes and gave the molecular formula $C_{53}H_{96}O_9$ by +ve FAB MS $[M]^+$ at m/z 876 (calcd 877.32), which was supported by its IR and NMR data. It showed UV absorption maxima (MeOH) at 264 nm, and IR absorption bands at 3437, 1722 and 1015 cm^{-1} for

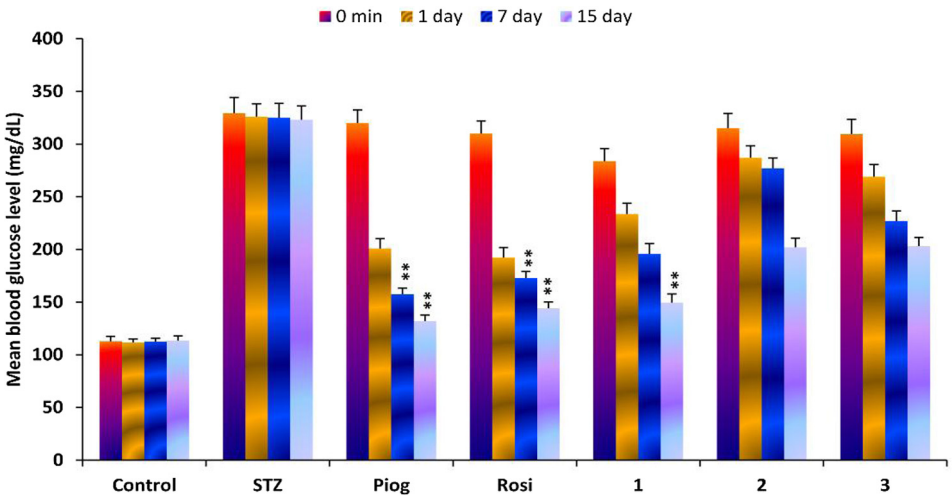

Figure 2 Effect of compounds **1**–**3** on blood glucose lowering in streptozotocin induced diabetic rats. Data is analysed by one way ANOVA followed by Dunnett's 't' test and expressed as mean ± SEM from five observations; ** indicates $p < 0.01$ vs diabetic control.

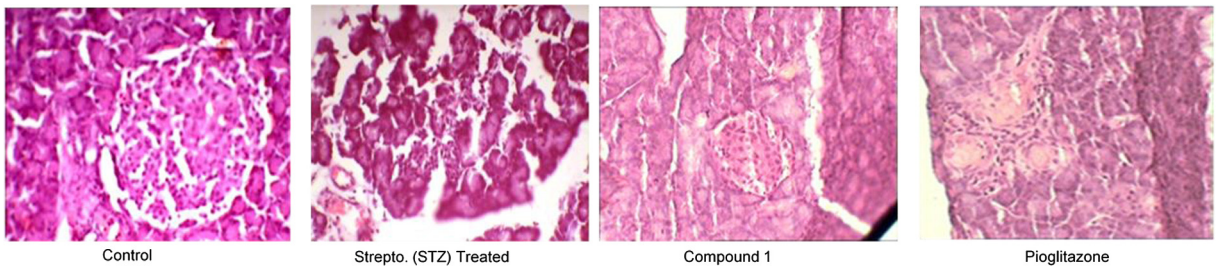

Figure 3A Histopathology report of rat pancreas. STZ treated groups showing reduce islet of Langerhans. Compound **1** and **pioglitazone** treated groups showing recovery of islet of Langerhans.

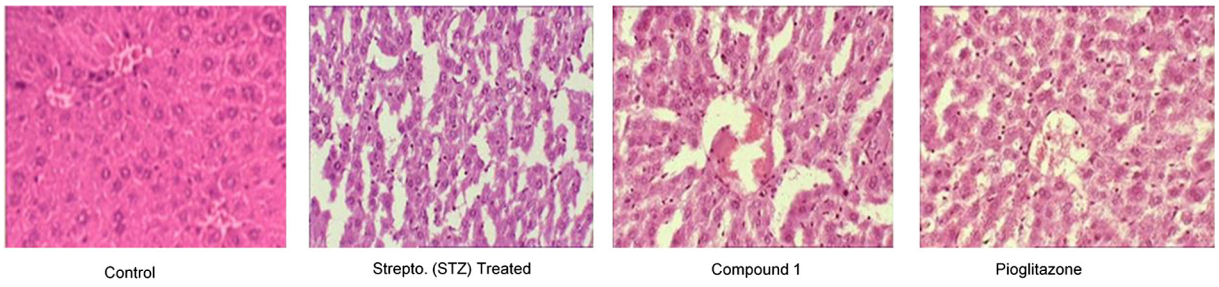

Figure 3B Histopathology report of rat liver showing normal arrangement of hepatocytes in the centrizonal area (Control). Compound **1** and **pioglitazone** treated groups showing normal arrangement of cells in the liver lobule and normal arrangement of hepatocytes in the centrizonal area. Strepto (STZ) treated groups showing perivenular inflammatory infiltration filling over the sinusoidal vacuolation of the hepatocyte nuclei.

hydroxy, carbonyl and ether functionalities, respectively. The signals in ^{1}H NMR and ^{13}C NMR spectra were similar to compound **2** except that it showed additional signals for a sugar moiety. The ^{1}H NMR revealed the characteristic anomeric signal (H-1″) as a doublet at δ_H 5.37 (J = 8.7 Hz). The H-2″ appeared as double doublet at δ 3.80 (J = 5.3, 6.1 Hz). The H-3″, H-4″ and H-5″ were observed as multiplets at δ 3.62, 3.35 and 3.92, respectively. The ^{13}C NMR of **3** were similar to compound **2** except that it exhibited five additional signals of the sugar unit at δ_C 108.11, 73.90, 79.94, 71.69 and 67.67 which were assigned to C-1″, C-2″, C-3″, C-4″ and C-5″, respectively (Aydogmus et al., 2006). Acid hydrolysis of **3** yielded an aglycone compound **2** and xylose sugar. The aglycone moiety was confirmed from mass spectrum showing fragment ion peak at m/z 744 for the molecular formula $C_{48}H_{87}O_5$. The position of glycosidation was confirmed by HMBC spectrum which showed a long range correlation of anomeric proton H-1″ (δ 5.37, J = 8.7 Hz) with C-4 (156.61) (Fig. 1). Based on these evidences, compound **3** was characterized as *2,3,4-trihydroxyphenethyl tetracontanoate-4-β-xylopyranoside*.

Table 1 ^{1}H (400 MHz, δ ppm) and ^{13}C NMR data (100 MHz, δ ppm) of compound **1**.

Positions	δ_H, J (Hz)	δ_C
2	–	163.60
3	6.57 (1H, s)	104.05
4	–	182.40
5	12.91 (1H, s, –OH)	162.38
6	9.92 (1H, s, –OH)	155.93
7	–	163.86
8	–	123.87
9	–	158.76
10	–	105.32
1′	–	123.75
2′&6′	7.83 (2H, d, J = 8.2 Hz)	127.99, 127.95
3′&5′	7.02 (2H, d, J = 8.8 Hz)	114.56, 114.46
4′	–	162.60
1″	3.85 (1H, t, J = 7.2 Hz)	89.33
2″	1.25 (2H, brs)	29.71
3″	2.21 (1H, m)	31.94
4″	0.88 (3H, d, J = 8.8 Hz)	8.57
5″	0.81 (3H, d, J = 8.4 Hz)	7.29
1″-OH	6.48 (1H,s)	–
4′-OMe & 7-OMe	3.92 (6H, s)	55.90, 55.52

3.2. Biological activity

The isolated compounds **1**–**3** were tested for *in vivo* antidiabetic activity in streptozotocin induced diabetic rats. Compound **1** significantly lowered blood glucose level to 149.92 mg/dl ± 8.63 ($p < 0.01$) in comparison with standard drugs pioglitazone (132 ± 5.02) and rosiglitazone (144 ± 6.3) after 15 days of study (Fig. 2). Compound **2** and **3** lowered blood glucose level to 202 mg/dl ± 9.72 and 203 mg/dl ± 9.92, respectively. The histopathological examination of the pancreas and liver of STZ-induced diabetic rats revealed extensive alterations. STZ caused significant damage to islets of langerhans of the pancreas showing markedly reduced islet cells, which were restored to near normal upon treatment with compound **1** and pioglitazone (Fig. 3). The liver of diabetic rats showed perivenular inflammatory infiltration filling over the sinusoidal vacuolation of the hepatocyte nuclei. The pathological changes observed in STZ-induced diabetes appeared closer to the normal after treatment with compound **1** and pioglitazone. It was observed that the compound **1** has the protective effect on the liver as well as the pancreas of the diabetic rats.

In order to validate the results of *in vivo* antidiabetic activity, the active compound **1** was docked for *in silico* studies against PPAR-γ target. PPAR-γ receptor has been found to be an important drug target for regulating fatty acid storage and glucose metabolism. On activation by ligands, this receptor leads to an increased insulin sensitivity and further glucose uptake. Molecular docking studies were done to provide insights of binding modes of molecules inside the large pocket of PPAR-γ receptors. It was observed that compound **1** showed glide core of -7.89 which is significantly higher than the glide score of standard drug Rosiglitazone (glide score of −5.77). Compound **1** was found to show π–π interaction with LYS 261 residue of the protein and is deeply buried into hydrophobic pocket of PPAR-γ receptor. The *in silico* ADME

Table 2 ^{1}H (400 MHz, δ ppm) and ^{13}C NMR data (100 MHz, δ ppm) of compounds **2** and **3**.

Positions	**2**		**3**	
	δ_H, J (Hz)	δ_C $CDCl_3$	δ_H, J (Hz)	δ_C, $CDCl_3$
1	–	130.05	–	131.25
2	9.42 (1H, s, –OH)	154.26	8.66 (1H, s, –OH)	154.76
3	10.82 (1H, s, –OH)	156.05	10.50 (1H, s, –OH)	155.15
4	11.58 (1H, s, OH)	156.21	–	156.61
5	6.76 (1H, d, J = 8.4 Hz)	115.33	6.76 (1H, d, J = 8.1 Hz)	116.32
6	7.07 (1H, d, J = 8.4 Hz)	129.99	7.08 (1H, d, J = 8.1 Hz)	129.69
7	2.85 (2H, t, J = 7.2 Hz)	34.38	2.85 (2H, t, J = 6.9 Hz)	34.98
8	4.23 (2H, t, J = 7.2 Hz)	64.97	4.23 (2H, t, J = 7.1 Hz)	64.77
1′	–	173.97	–	173.07
2′	2.27 (2H, t, J = 7.6 Hz)	34.29	2.40 (2H, m)	34.19
3′	1.60 (74 H, brs, 37 × CH_2)	31.94–22.71 (37 × CH_2)	1.63 (74 H, brs, 37 × CH_2)	31.74–22.61 (37 × CH_2)
Me	0.88 (3H, t, J = 6.3 Hz, Me-40′)	14.41	0.85 (3H, t, J = 6.1 Hz, Me-40′)	14.41
1″	–	–	5.37 (1H, d, J = 8.7 Hz)	108.11
2″	–	–	3.80 (2H, dd, J = 5.3, 6.1 Hz)	73.90
3″	–	–	3.62 (1H, m)	79.94
4″	–	–	3.35 (1H, m)	71.69
5″	–	–	3.92 (2H, m)	67.67

Table 3 Docking score of compound **1**.

Ligands	G-score	Glide energy	Log P O/W	PSA	Log S
1	−7.89	−38.38	3.313	102.13	−5.785
Rosiglitazone	−5.77	−71.55	3.475	94.37	−4.497

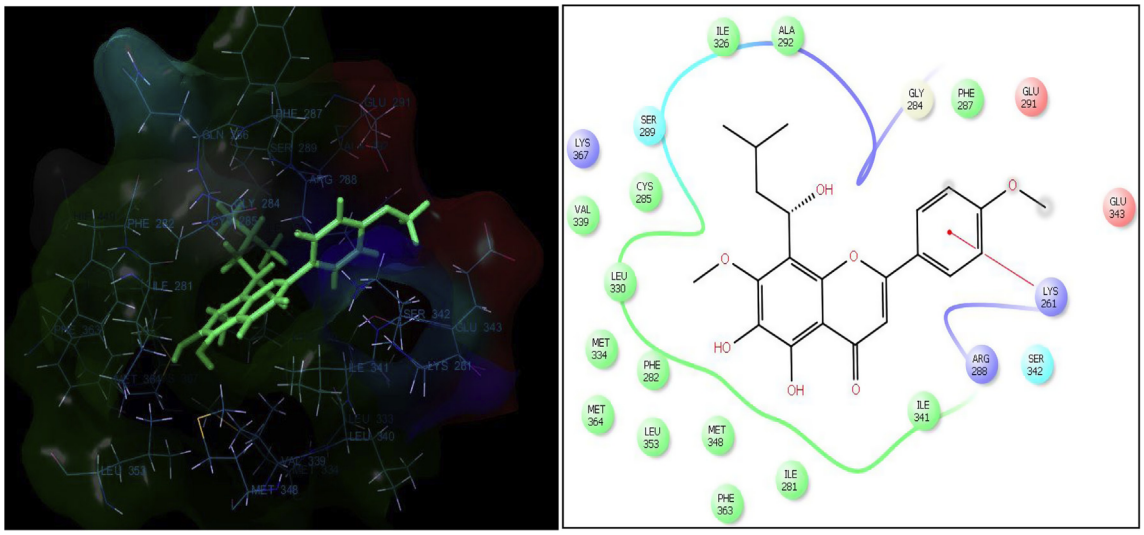

Figure 4 Molecular docking of compound **1** showing interaction PPAR-γ receptor.

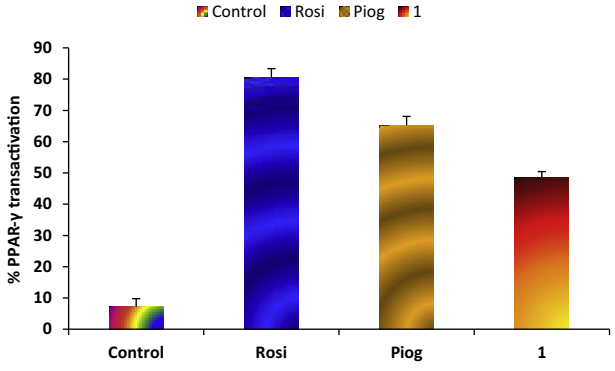

Figure 5 PPAR-γ transactivation activity of compound **1**. Values are expressed as mean ± SEM from three experiments conducted in triplicate at 10 μM.

(Absorption, Distribution, Metabolism and Excretion) prediction of compound **1** was found to be within the acceptable range. The calculated glide score, binding energies and predicted ADME of compound **1** are presented in Table 3 and Fig. 4. In order to confirm the mechanism of action the compound **1** was evaluated for *in vitro* PPAR-γ transactivation activity. It was found to exhibit moderate *in vitro* PPAR-γ transactivation activity of 48.52% in comparison with the standard drugs Rosiglitazone and Pioglitazone, which showed 80.47% and 65.27% transactivation activity, respectively (Fig. 5).

4. Conclusion

In the present study, one new flavone and two new phenolic esters were isolated from *C. lanceolatus* and subjected to evaluation of their anti diabetic potential. Compound **1** exhibited significant *in vivo* blood glucose lowering effect in STZ induced diabetic rats without causing any toxicity to the liver and pancreas. Compound **1** exhibited a glide score of −7.89 against PPAR-γ target in molecular docking studies which is significantly higher than that of reference molecule rosiglitazone (glide score of −5.77). It also exhibited moderate *in vitro* PPAR-γ transactivation activity of 48.52% in comparison with the standard drugs Rosiglitazone and Pioglitazone, which showed a transactivation activity of 80.47% and 65.27% respectively. Compound **1** may have exerted the antidiabetic effect by activating PPAR-γ receptors.

Acknowledgements

The authors thank Vice Chancellor, Dr. G. N. Qazi, Jamia Hamdard, for providing all the necessary facilities to the Department of Chemistry. Syed Nazreen acknowledges University Grants Commission, India for providing financial assistance.

Appendix A. Supplementary data

Supplementary data associated with this article can be found, in the online version, at http://dx.doi.org/10.1016/j.arabjc.2014.11. 029.

References

Anonymous, 1992. The Wealth of India 3, 64–65.
Aydogmus, Z., Yesilyurt, V., Topcu, G., 2006. Nat. Prod. Res. 20, 775–781.
Boue, M.S., Carter-Wientjes, H.C., Shih, Y.B., Cleveland, E.T., 2003. J. Chromatogr., A 991, 61–68.
Chistokhodova, N., Nguygen, C., Calvino, T., Kachriskaia, I., Cuuingham, G., Miles, D.H., 2002. J. Ethnopharmacol. 82, 277–280.
Dahlqvist, A., 1961. Biochem. J. 80, 547–551.
Gomber, C., Saxena, S., 2007. CEJ Med. 2, 79–88.
Huq, F., Misra, L.N., 1997. Planta Med. 63, 369–370.
Kobayashi, K., Ishihara, T., Khono, E., Miyase, T., Yoshizaki, F., 2006. Biol. Pharma. Bull. 2, 1275–1277.
Nazreen, S., Kaur, G., Alam, M.M., Haider, S., Shafi, S., Hamid, H., Alam, M.S., 2011. Pharmacologyonline 1, 799–808.
Nazreen, S., Kaur, G., Alam, M.M., Shafi, S., Hamid, H., Ali, M., Alam, M.S., 2012. Fitoterapia 83, 1623–1627.

Sangwan, N.K., Verma, B.S., Verma, K.K., Dhindsa, K.S., 1990. Pestic. Sci. 3, 331–335.
Saxena, S., Gomber, C., 2006. Pharm. Biol. 3, 194–201.
Wollenweber, E., Wehde, R., Dorr, M., Lang, G., Stevens, J.F., 2000. Phytochemistry 55, 965–970.
Wrigley, J.W., Fagg, M., 1993. Bottlebrushes, Paperbarks and Tea Trees and all other plants in the Leptospermum alliance. Angus & Robertson, Sydney, Australia, p. 352.
Younes, M.E., 1975. Phytochemistry 14, 592.